EurJIC European Journal of Inorganic Chemistry

ChemPubSoc Europe

FULL PAPER

DOI:10.1002/ejic.201400027

Sodium "Activation" of Silano-Phosphonate Modified Mesoporous TiO_2 Leading to Improved Rare-Earth Element Extraction

Mícheál P. Moloney,*[a] Jérémy Causse,[a] Cedric Loubat,[b] and Agnès Grandjean[a]

Keywords: Waste prevention / Mesoporous materials / Cations / Titanates / Lanthanides / Cerium

Due to their presence in most modern electronic devices and as waste products in the nuclear cycle, a great deal of interest has been generated in the acquisition and/or recycling/removal of rare-earth elements (REE). Here, we present a simple one-pot route for the preparation of dimethylphosphatoethyltriethoxysilane (SiP) functionalised mesoporous TiO_2 particles. The resistance of TiO_2 to strong bases allowed for the use of NaOH to "activate" the phosphonate head group of the functionality, significantly improving its efficiency. Levels of 92.6 mg/g Ce^{3+} were extracted from water, which is double the previously reported value for the extraction of REEs with this type of extractant. SiP-TiO_2 (Na) was also used to separate completely the Ce^{3+} from aqueous solutions containing Sr^{2+} and Cs^{+}. Finally, the nanocomposite separated Ce^{3+} from other homovalent REEs, for example, Yb^{3+} (1:1.4 separation ratio).

Introduction

Rare-earth metals have become increasingly important over the last several decades. This is due to their use in both the electronics and the biomedical industries,[1–4] as well as the use of their compounds in catalysis,[5,6] nanotechnology,[7,8] the production of luminescence compounds,[9,10] and various chemical engineering applications.[2,11] Rare-earth elements (REE) can therefore be found in a variety of products from audio-visual devices such as mobile phones, televisions and computer displays, to energy storage devices such as long-life batteries.[12,13] Cerium is also used by the automotive industry in catalytic converters, and by the petroleum industry in refining as a cracking catalyst.[12,13] These varied uses make having a constant and reliable source of pure REE important. However, despite the relative abundance of these so called "rare earths" (Ce is the 25th most abundant metal in the Earth's crust, with a concentration comparable to copper) they are still relatively expensive because both their production level and use have varied over the last decade.[14] These variations are due, in the most part, to environmental and geo-political considerations combined with an increasing demand for high-end electronic goods.[15] It is with these factors in mind that reliable sources of REE are now being sought. The recent advances in recycling technology as well as the ever-decreasing "shelf life" of modern electronic devices have made the idea of device recycling and REE recuperation more popular. It should also be noted that as the demand for REE begins to outstrip their production, the idea of device recycling begins to be economically viable.[16]

While recycling is clearly very important, large volumes of REEs are still acquired from mining their ores. However, lanthanide-containing ores are normally found as mixtures of various REEs, for example, Bastnasite (Ce,La,Y)COF, and Monazite-(Ce) $(CeLaNdTh)PO_4$.[17] This poses a problem because the separation of mixtures of REEs can prove difficult due to a phenomenon known as lanthanide contraction. This property causes a relatively gradual decrease in ionic size with increasing atomic number, giving the various REEs similar sizes, which makes them difficult to separate. In the following article, we propose the use of mesoporous TiO_2 modified with a silano-phosphonate compound to do just this, i.e., separate lanthanides. While organic resins are well-known for their ability to remove REEs from solution, their propensity to swell and explode in strong acid (an integral component of the mining process) makes these inorganic TiO_2 nanocomposites a safer option.[17a]

Lanthanides are also often used to model actinides, and are themselves present in nuclear waste.[17b] In these scenarios, inorganic extracts are again better than organic ion ex-

[a] Laboratoire de Nanomatériaux pour l'Energie et le Recyclage, Institut de Chimie Séparative de Marcoule, Centre de Marcoule, Bât. 426,
BP 17171, 30207 Bagnols-sur-Cèze Cedex, France
E-mail: molonem@tcd.ie
http://www.icsm.fr/
[b] Specific Polymers,
Avenue des Cocardieres, 34160 Castries, France
E-mail: cedric.loubat@specificpolymers.fr

Supporting information for this article is available on the WWW under http://dx.doi.org/10.1002/ejic.201400027

changers because they are effected to a lesser degree by radionuclides and radiation.[17b] Whereas SiO_2 is a more common support for $(EtO)_3SiR$ based functionality, it was not the support of choice in this work; instead, we report for the first time TiO_2 functionalised with SiP. The choice of TiO_2 was initially made because we wished to model a type of TiO_2 membrane that is industrially significant.[11,18–20] However, TiO_2 proved to be unexpectedly advantageous because it allowed for the use of concentrated NaOH(aq.) in the "activation" of the SiP functionality. We use the term "activation" and not hydrolysis for two reasons. First, ^{31}P MAS-NMR analysis demonstrated that a significant number of the SiP P-OCH_3 groups were already hydrolysed by a hydrothermal process employed in this work. Second, despite this hydrolysis, it was not until the NaOH treatment that a marked difference in the extraction ability of SiP-TiO_2 over that of unfunctionalised TiO_2 was seen. Activation with NaOH(aq.) proved to be far more effective than with the more common acid (HCl) hydrolysis recommended in the literature.[21] Such NaOH treatment would have not been possible with a silica-based support due to the high solubility of silica in strong base.

It should also be noted that TiO_2 is an amphoteric material, and this property has been used to assist in the uptake and release of ions from solution.[22–28] It was also believed that this property would also prove to be useful in this work by assisting in the recovery of the sorbed metals. When recovery the collected metals was desired, simply lowering the pH to 3 led to release of 80% of those sorbed metals.

The TiO_2 particles used in this work were prepared as described in the literature.[29,30] It should be noted that although the hydrothermal process recommended in the literature was found to decrease rather than increase the specific surface area of the TiO_2, it was still retained in this work. This process was kept for two specific reasons. First, it was an effective method for the removal of surface-bound ethylene glycol. Second, it allowed us to demonstrate the effectiveness of the NaOH activation process by hydrolysing the P-OCH_3 groups without the need for strong acid. SiP was added to the Ti precursor before particle formation, which was done to ensure maximum surface coverage. Although it has been extensively reported (and was an initial concern here) that a phosphonate group containing silane such as SiP would strongly coordinate to the Lewis acid surface sites of TiO_2 through its phosphonate oxygen, this was found not to be the case.[31] ^{13}C MAS-NMR analysis carried out in this work showed that the majority of the P-OCH_3 methyl protecting groups present on the phosphonate head of the SiP functionality were still present after particle formation. The majority of these remaining protecting groups were only hydrolysed by hydrothermal treatment, which took place after particle formation. More importantly ^{31}P and ^{39}Si MAS-NMR analysis showed, respectively, not only the absence of peaks from Ti-O-P but also the presence of Ti-O–Si bonds.[32,33] These results confirmed that the silane tail group, and not the phosphonate head group, was the point of SiP attachment on the TiO_2.

The sorbants used in this study were all nitrates, with the exception of $GdCl_3$. This salt was used to determine the effect, if any, of changing the counterion on the absorbance rate of Gd^{3+} onto the modified SiP-TiO_2 particles. In total four REEs nitrates were examined Ce, Nd, Gd and Yb, with the focus being placed on Ce and the effect, if any, of the presence of the other REEs on Ce sorbance. The effects of the presence of M^+ (Cs) and M^{2+} (Sr) on Ce^{3+} sorbance were also studied. Kinetic sorption studies as well as isotherm sorption experiments allowed the sorption mechanism used by this material to be determined.

Lastly and perhaps most interestingly, it should also be noted that previous studies with the commercially available ethyl analogue of SiP grafted onto silica have shown the ability of this molecule to sorb REEs to be no greater than ca. 0.3 mmol/g.[11] In fact, our own studies of Ce and Nd found this to be lower still: 0.17 mmol/g. However, the use of a TiO_2 support and consequently the ability to use sodium activation allowed us to more than double this value (Ce^{3+} 0.66 mmol/g, Gd^{3+} 0.76 mmol/g and Yb 0.79 mmol/g).

Results and Discussion

Characterisation of SiP-TiO_2

The SiP-TiO_2 was characterised by environmental scanning electron microscopy (ESEM), nitrogen isotherm adsorption, small-angle X-ray scattering (SAXS) and magic-angle spinning NMR (MAS-NMR) spectroscopy. ESEM showed the presence of large spherical particles, MAS-NMR confirmed the presence and structure of the SiP. Nitrogen isotherm adsorption showed a high surface area and confirmed that the particles were mesoporous. SAXS measurements showed, as expected, no specific arrangement of the pores (see the Supporting Information). The functionalised TiO_2 will be referred to as SiP-TiO_2 with (BH), (AH) and (ANa) being used to denote before and after hydrothermal treatment, and after sodium treatment, respectively.

ESEM Analysis

In Figure 1 ESEM images of SiP-TiO_2 before (BH) and after (AH) the hydrothermal treatments are shown. The process causes a slight increase in particle size, monodispersity, and surface roughness, due to Oswalt ripening.[29] Initially, the (BH) particles are "smooth" surfaced and spherical with little aggregation, and a size distribution of 366 nm ± 57 nm, (Figure 1, a). However, this changed once they were subjected to the hydrothermal treatment (6 h at 120 °C). The smaller TiO_2 (AH) particles aggregated on the surfaces of the larger particles causing them to become visibly rougher. This caused the size, and the size distribution, of the particles to change to 399 ± 52 nm, (Figure 1b and c).

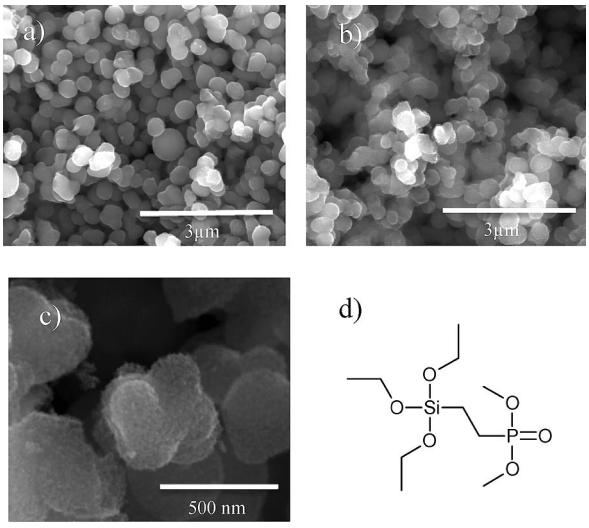

Figure 1. ESEM images of SiP-TiO_2 (a) before, and (b and c) after hydrothermal treatment. (d) Depiction of the SiP functionality.

Nitrogen Isotherm Adsorption Analysis

The hydrothermal treatment was initially performed to increase the specific surface area by creating mesopores.[29] However, N_2 isotherm adsorption measurements showed that this was not the case; the (BH) particles were already mesoporous, and the hydrothermal process lowered rather than increased the specific surface area (see the Supporting Information). SiP-TiO_2 (BH) and (AH) were found to have specific surface areas of 331 and 249 m^2/g, respectively. Control experiments performed on unfunctionalised TiO_2 showed 331 and 235 m^2/g for BH and AH, respectively, thereby demonstrating that this diminishing effect was not a result of the presence of the SiP. The pore size and pore volume of the SiP-TiO_2 particles was found to be roughly half that of the unfunctionalised TiO_2, which is likely due to the presence of the SiP functionality within the pores. It should also be noted that whereas hydrothermal treatment did indeed cause an increase in the pore size of the unfunctionalised TiO_2, a decrease was seen for the SiP-TiO_2. This decrease was probably due to the further hydrolysis and cross-linking of the SiP within the pores, 3.9, 4.1 and 2.8 nm for BH, AH and ANa, respectively. This was backed-up by the change in the structure of the ^{39}Si MAS-NMR peaks for BH and AH (Figure 3 and the Supporting Information).

MAS-NMR Analysis

^{29}Si, ^{13}C, and ^{31}P MAS-NMR analyses were used to confirm the presence and to examine the structure of the bound SiP molecule (Figures 2, 3 and 4). ^{29}Si MAS NMR analysis of the SiP-TiO_2 (AH) showed a series of complex overlapping signals between –40 and –70 ppm (Figure 2). The peaks at –41 and –45 ppm confirm the presence of Ti-O–Si bonds. This observation, combined with the ^{13}C MAS-NMR spectroscopic data (Figure 3), and absence of Ti–O–P signals in the ^{31}P MAS-NMR spectrum (Figure 4), confirmed that the silane tail was the sole point of attachment for the SiP on the TiO_2 surface. Several doublets ($J_{P,Si}$ = 36.5 Hz) representing the SiP molecule in various states of cross-linkage were also present (Figure 2 and Table 1).[33,34] Considering the high degree of intermolecular reactively seen in silanes, and that very similar ^{29}Si MAS NMR spectroscopic data has been reported for the ethyl analogue of SiP, the presence of these peaks was expected.

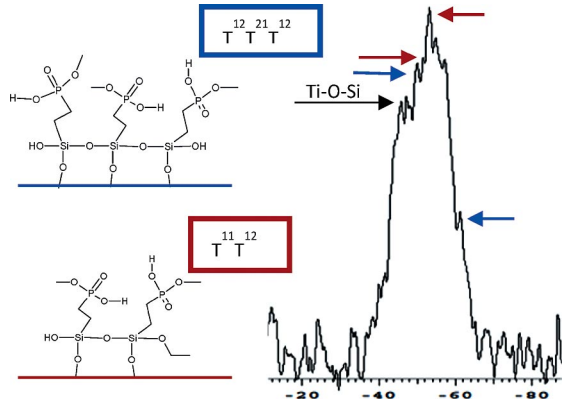

Figure 2. Right: ^{39}Si MAS-NMR spectrum of SiP-TiO_2 (AH). The peaks at δ = –41 and –45 ppm are indicative of Si–O–Ti bonds. The remaining peaks indicate extensive intermolecular polycondensation has taken place. Left: Drawing of the SiP in its $T^{12}T^{21}T^{12}$ (blue) and $T^{11}T^{12}$ (red) structures, with corresponding arrows indicating their peak positions.[34] The coloured base lines represent the TiO_2 surface.

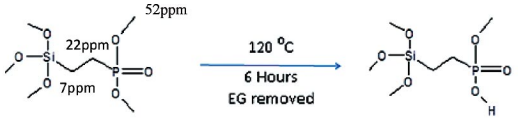

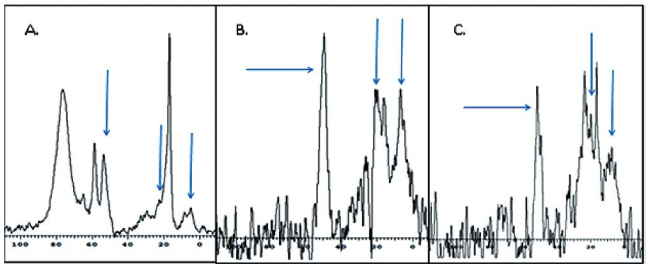

Figure 3. Top: TiO_2-bound SiP before and after hydrothermal treatment. Note silica oxygen atoms are bound to the TiO_2 surface. Bottom: ^{13}C MAS-NMR spectra of SiP-TiO_2 before and after hydrothermal treatment (A and B, respectively), and after treatment with NaOH (C). The blue arrows indicate the positions of the SiP carbon atoms (δ = 7, 22 and 52 ppm). The drop in relative intensity of the peak at δ = 52 ppm indicates that some of the corresponding P-O-CH_3 groups have been hydrolysed. Note the absence of the methyl (δ = 20 ppm), EG (δ = 59 ppm) and PEG (δ = 79 ppm) peaks after the hydrothermal process (B and C). The presence of other peaks in (C) at δ = 18 and 24 ppm may be due to the photocatalytic breakdown of the SiP.[32]

Whereas the SiP molecule is indeed bound to the surface through the silica tail, it is likely that it is not present as individual molecules bound through its three Si-O oxygen

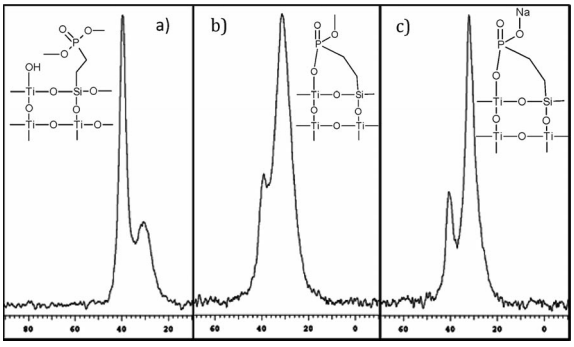

Figure 4. ^{31}P MAS-NMR spectra of (a) SiP-TiO_2 BH, (b) AH, and (c) ANa. The structural insets represent the possible structure of the majority of the surface SiP for that particular NMR spectrum. The peak at δ = 40 ppm is believed to be unhydrolysed SiP, whereas the peak at δ = 30 ppm is the hydrolysed analogue. The sharper version of the 30 ppm peak in spectrum (c) is due to presence of sorbed Na^+ ions.

Table 1. ^{39}Si MAS-NMR peak assignments for monomeric and oligomeric species obtained from the hydrolysis of SiP.[34] The OH represent oxygen atoms that are bonded to the TiO_2 surface.

Structure	Formula	Reference [ppm]	Result [ppm]
$RSi(OH)_3$			
$RSi(OH)_2(OEt)$	T^{03}	–42.4	–42
$RSi(OH)(OEt)_2$	T^{02}	–43.7	–43
$RSi(OEt)_3$	T^{01}	–45.4	n/a
$R(OH)_2SiOSi(OH)$-	T^{00}	–47.4	–48
-$(R)OSi(OH)_2R$	$T^{12}T^{21}T^{12}$	–51.2	–54
$R(OH)_2SiOSi(OH)_2R$		and –60.4	and –61
$R(OH)(OEt)SiOSi(OH)_2R$	$T^{12}T^{12}$	–51.3	–52
	$T^{11}T^{12}$	–51.5	–54
		and –52.8	and –53

groups. Instead, it is present either as islands or as interconnecting layers spread across the TiO_2 surface. The presence of branched multiple layers must also be considered. These factors make calculating the number of SiP molecules on the surface quite challenging. However, as long as the phosphonate head groups are visible in solution, this intermolecular polycondensation should not (and does not) diminish the ability of the molecule to sorb target metals.

^{13}C MAS-NMR analysis of SiP-TiO_2 (BH) confirmed the presence of the SiP molecule, with characteristic peaks at 7, 22 and 52 ppm (Figure 3, A). Although the P-OCH_3 (δ = 52 ppm) peak continues to be present in the SiP-TiO_2 (AH) and (ANa) samples, its size relative to the other SiP peaks continually diminishes from double the size of the other SiP peaks (7 and 22 ppm) in the BH sample to roughly the same in the AH and less in the ANa samples (Figure 3, b and c, respectively). Although peak integration in ^{13}C MAS-NMR spectra is not as precise as in ^{1}H NMR spectra, the almost equal intensities of the peaks at δ = 7 and 22 ppm (which correspond to only one C apiece) and the peak at δ = 52 ppm (which corresponds to the two methyl-carbons), indicates that phosphonate hydrolyses has taken place, to a large degree, during the hydrothermal treatment. Another striking feature of the SiP-TiO_2 ^{13}C MAS-NMR spectra of (BH) and (AH) is the removal of the ethylene glycol (EG) by the hydrothermal process.

The ^{13}C MAS-NMR spectrum of SiP-TiO_2 (BH) shows that the various washings and ethanol Soxhlet extraction did not remove all the EG, as seen by the presence of the EG peak at δ = 59 ppm. However, this peak was not present after the hydrothermal (HT) process.

The difficulty in removing the EG indicates that it is bound to the TiO_2 surface. This is not surprising because the EG acted as both the solvent and as a co-stabiliser during TiO_2 formation. The presence of a strong peak at δ = 75 ppm (BH) indicates that the EG underwent polymerisation on the TiO_2 surface to form PEG, however, this was also removed during the HT process. The disappearance of the EG and PEG peaks in the ^{13}C MAS-NMR spectrum of SiP-TiO_2 (AH) (i.e., after heating to reflux in water) demonstrated that the hydrothermal process was an effective and simple method with which to clean the particles (Figure 3, B). The alkane contamination at δ = 17 ppm was also removed by the hydrothermal process, which indicated the continued hydrolysis of any remaining Si-O-R groups. Finally, and serendipitously, the hydrothermal process proved sufficient to hydrolyse the phosphonate P-O-CH_3 groups without needing to heat the particles to reflux in concentrated HCl, as recommended in the literature.[21] For this reason, the hydrothermal process was retained, despite the detrimental affect the process had on the specific surface area of the SiP-TiO_2.

The absence of Ti-O-P peaks in the ^{31}P NMR spectra indicates that the phosphonate is not used to anchor the SiP to the TiO_2 surface. The ^{31}P MAS-NMR spectrum of SiP-TiO_2 (BH) shows two signals, a dominant signal at δ = 41 ppm and a second at δ = 31 ppm with a peak height ratio of 3.14:1 (Figure 4). Because the ^{31}P NMR spectrum of the free SiP molecule in $CDCl_3$ shows a single peak at δ = 36 ppm (see the Supporting Information), we can assume that the second peak is due to the creation of a second distinct phosphorus environment.[21] This shift in the position of the original peak from δ = 36 to 41 ppm, as well as the appearance of a second peak at δ = 31 ppm, was expected because similar results have been reported by Pan et al.[21] The peak at δ = 41 ppm was assigned to unhydrolysed [$PO(OR)_2$], or partially hydrolysed [PO(OR)(OH)] SiP; its shift from δ = 36 to 41 ppm is probably due to its grafting onto the TiO_2 surface.[21] The second peak at δ = 31 ppm was due to another distinct phosphorus environment being formed when the –OH on the partially hydrolysed phosphonate groups formed hydrogen surface bonds with the –OH groups present on the substrate (Figure 4, b, insets). It should be noted that whereas Figure 4 (a) shows that the SiP underwent partial hydrolysis during particle formation, as mentioned earlier, the lack of Ti-O-P peaks in the ^{31}P NMR spectrum confirms that the phosphonate is not used to anchor the SiP to the TiO_2 surface. The ^{31}P MAS-NMR spectrum of SiP-TiO_2 (AH) showed a stark reversal in the intensities of the two peaks. Once the particles were treated hydrothermally, the intensities of the peaks inverted (1:2 intensity for peaks at δ =40 and 30 ppm, respectively; Fig-

ure 4, b). This inversion is a result of the hydrolysis of the majority of the P-OR to P-OH groups, and the subsequent interaction of these P-OH groups with the TiO_2 surface. Sodium treatment causes the peak at δ = 31 ppm to strengthen further (peak intensity ratio at 40/31 ppm, 1:2.4; Figure 4, c). This increase is a result of the continued hydrolysis of the P-O-CH_3 to P-OH groups. The peak at δ = 31 ppm not only increases in intensity, but it also narrows substantially. This sharpening effect indicates the increased uniformity of the chemical environment, for example, instead of a mixture of partially and fully hydrolysed groups (Figure 4, b, inset), only completely hydrolysed groups are observed (Figure 4, c, inset). The sharpening may also be due to the presence of the Na^+ on the SiP molecules.[35] Because these particles were washed until neutral after the NaOH treatment, we believe that these Na^+ ions have been sorbed by the SiP-TiO_2. The presence of Na^+ ions on the SiP-TiO_2 was later confirmed when they were detected by chromatography after being displaced by the target metals during sorption studies. This Na sorption process proved invaluable because it greatly improved the ability of the SiP-TiO_2 (ANa) to remove other metals from the liquid effluent (see below).

Sorption Studies

Initial Tests

Preliminary studies were carried out to determine whether changing the ionic strength or pH would affect the uptake of target metals. However, it was found that the inclusion of a large excess of $NaNO_3$ had no effect on the SiP-TiO_2 ability to sorb the target metals (details not shown). All studies included here were carried out at pH 6.4–6.8. However, the pH was seen to fall to around 5.8 by the end of each experiment. Further pH studies were carried out but are not included. Above pH 7.6 the metal nitrate salts formed insoluble hydroxides and therefore could not be sorbed. Studies carried out at pH 3 resulted in almost identical sorption plots but with a 50% drop in the concentration of metal sorbed. Ce sorbtion tests were carried out on both SiP-TiO_2 (AH) and unfunctionalised TiO_2 (AH). By comparing SiP-TiO_2 (AH) with unfunctionalised TiO_2 (AH), as a control, it was possible to: (a) observe whether TiO_2 itself had any affinity for Ce^{3+}, and (b) determine the ability of the SiP molecule to sorb Ce^{3+} ions. Surprisingly, however, it was found that the difference between the unfunctionalised TiO_2 (AH) and SiP-TiO_2 (AH) was negligible. The unfunctionalised TiO_2 (AH) sorbed 22 mg Ce per gram of TiO_2, whereas the SiP-TiO_2 (AH) was only slightly above this (29 mg/g). These results were found to be almost identical to those observed for Ce^{3+} sorbed onto both plain and SiP functionalised SBA-15 (literature standard) when the results were normalised for molar mass (see the Supporting Information). Therefore, it appeared that the presence of the SiP functionality seemed to make little difference on the sorbtion properties of the TiO_2 (AH). This was surprising because (a) this molecule has been previously reported to have an affinity for lanthanides, and (b) as previously mentioned, the ^{31}P MAS-NMR spectra (Figure 4, b) showed a high concentration of P-OH groups on the SiP-TIO_2 (AH) surface.[11] In an attempt to improve upon these results, the SiP-TiO_2 (AH) particles were heated to reflux in 12M HCl (as recommended in the literature).[21] This was done to hydrolysis any remaining P-OCH_3 groups. However, this acid reflux diminished, rather than enhanced, the ability of the SiP-TiO_2 to sorb Ce^{3+}.

NaOH Treatment

Because acid treatment proved to be detrimental to the sorbtion properties of the SiP-TiO_2 (AH), base treatment was performed; this cannot usually be done because traditional silica supports are easily solubilised by strong bases. Briefly, SiP functionalised mesoporous TiO_2 (AH) was dispersed and stirred in concentrated aqueous NaOH (15 g/L), then collected by centrifugation after an hour and washed until pH neutral. The particles showed a marked improvement in their ability to sorb metals. Control experiments were carried out by using unfunctionalised TiO_2 (ANa) to determine whether this increase in sorbance was due to the NaOH having an effect on the SiP or on the TiO_2 itself. Absorption isotherms were carried out using Ce^{3+} with TiO_2 (AH) and (ANa) and SiP-TiO_2 (AH) and (ANa) (see the Supporting Information). The NaOH wash had little effect on the unfunctionalised TiO_2, whereas the maximum sorption capacity of the functionalised SiP-TiO_2 increased by a factor of three. This demonstrated that NaOH treatment affected the SiP and not the TiO_2 groups.

Although this enhancement may be due to base hydrolysis of any remaining surface P-O-CH_3 groups, we believe that this is not the case for the three following reasons: (i) ^{31}P MAS-NMR analysis (Figure 4, b) revealed the presence of a large number of P-OH groups after hydrothermal treatment. The relatively small change in the intensities of the ^{31}P MAS-NMR peaks after NaOH treatment suggests that the number of hydrolysed phosphonate groups remains, to a large extent, unchanged. (ii) As previously mentioned, acid treatment was performed by heating the SiP-TiO_2 (AH) particles to reflux in 12M HCl in an attempt to hydrolysis any remaining P-OCH_3 groups.[21] However, this proved to have no positive effect on the metal uptake. In fact, the acid reflux diminished, not enhanced, the ability of the SiP-TiO_2 to sorb Ce^{3+}, indicating again that the degree of hydrolysis of SiP is no longer a factor. (iii) SiP-TiO_2 (AH) and acid-treated SiP modified SBA-15 showed almost identical sorption results, indicating again the degree of hydrolysis is not a factor (see the Supporting Information).

Taking the three points detailed above into account, it would seem that 30 mg/g (as seen in the previous section) is the maximum Ce^{3+} sorption capacity for a support functionalised with hydrolysed SiP, without NaOH treatment. We therefore concluded that the increased sorbance of target metals onto SiP-TiO_2 after NaOH treatment was not due to an increase in the number of hydrolysed P-OCH_3 sites but, rather, due to the formation of the P-ONa groups on the TiO_2 surface. Alkoxides (R-ONa) are more basic

than alcohols (R-OH) with pK_a values of >15 and <5, respectively. Therefore, we believe that the increased affinity of the SiP-TiO_2 (ANa) for Ce^{3+} (and other weakly acidic metal salts) is a result of this higher basicity due to the presence of more easily exchangeable Na^+ ions on the SiP-TiO_2. As previously mentioned, the sharpening of the ^{31}P MAS-NMR peaks (Figure 4, c) indicates the presence of metal ions bound to the phosphonate.[35] Because the SiP-TiO_2 (ANa) particles were washed until neutral, any sodium present must have been sorbed. During the sorbtion studies ion chromatography showed that milliequivalent amounts of Na^+ were released as other metals Cs^+, Sr^{2+} and Ce^{3+} were sorbed by the SiP-TiO_2 (ANa) (Figure 5). This confirmed not only the presence of Na on SiP-TiO_2 but also its facilitation of the sorption of other metals through an ion-exchange mechanism onto the SiP-TiO_2 (ANa).

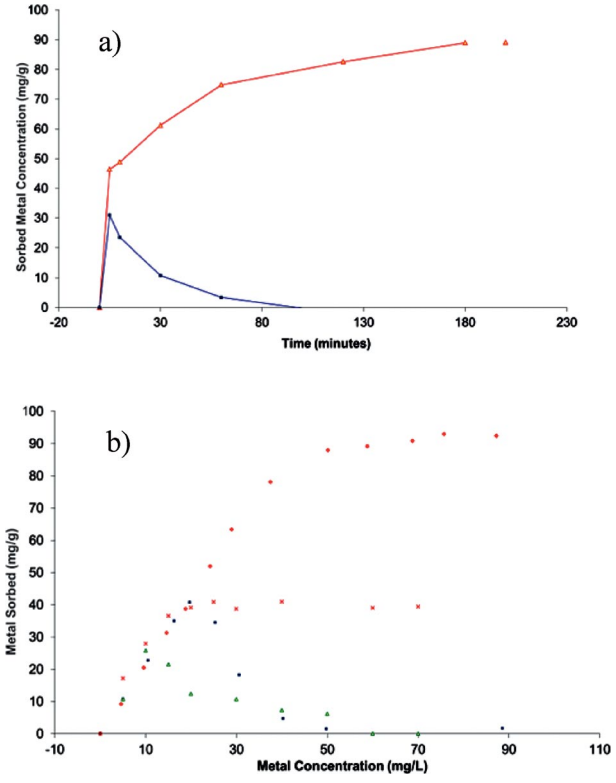

Figure 5. (A) Effect of stirring time on the sorption of Ce^{3+} (red) and Sr^{2+} (blue) onto SiP-TiO_2 (ANa). Initial Sr sorbance was reversed within the first 15 min. (B) Sorption isotherm of Ce (red diamonds), Sr (blue squares), and Cs (green/yellow triangles) solution on SiP-TiO_2 (ANa). The red x symbols represent the Na^+ released by the SiP-TiO_2 (ANa) as it absorbed the other metals.

Cerium Sorption Studies – Kinetics

Initial separation studies with SiP-TiO_2 (ANa) were carried out to determine whether Ce^{3+} could be separated from a mixed solution of di- and monovalent metals. The industrially significant elements strontium and caesium were chosen as M^{2+} and M^+, respectively. The pH was measured (as with all sorption experiments presented here) at t = 0 and at equilibrium. The pH was found to decrease slightly over the course of the experiments from pH 6.4 to around 5.8. Both kinetic experiments and adsorption isotherms were carried out. The kinetic experiments were performed by first sonicating SiP-TiO_2 (ANa) (20 mg) in deionised water (20 mL) for 30 min or until it was completely dispersed. This dispersion was then added to a 100 mL mixed solution of the three metal nitrates (≥ 20 mg/L each) in deionised water. Samples were taken at set intervals over a 6 h period and then they were filtered using 200 nm Whatman hydrophilic filters to remove the SiP-TiO_2. The metal concentration in the filtrate was examined by ICP analysis. It should be noted that 50% of the total amount of cerium sorbed took place in the first five minutes (Figure 5, a). Sr^{2+} was also initially sorbed within the first five minutes but this was quickly reversed and the metal was released. These results revealed that, although the ligand was not charge specific, in a high concentration competitive environment, previously sorbed Sr^{+2} ions are quickly released and replaced by any Ce^{3+} ions remaining in the solution. This phenomenon is also true for Cs^+ ions. As with the Sr^{2+}, caesium was sorbed in the early stages of the process, but then released (Figure 5, b).

Cerium Sorption Studies – Langmuir Isotherms

The adsorption isotherm plot of the previous system, now with the Caesium and Sodium data included, is given in Figure 5 (b). Each point on the Langmuir curve represents a different experiment, which was performed by stirring 4 mg of well-sonicated SiP-TiO_2 (ANa) overnight in a metal nitrate solution of defined concentration. At low concentrations the particles sorb all three metals indiscriminately. However, as the concentrations of the metals were increased a point was reached where only the Ce^{3+} was sorbed. That is to say, Ce^{3+} was preferentially sorbed over the other metals. Measurement of the equilibrium Na^+ concentration at each point of the adsorption isotherm showed an increase in the sodium concentration as the target metal concentrations were increased; this continued until eventually the Na concentration plateaued at 40 mg/g (Figure 5, b). It should be noted that ion chromatography of the initial metal nitrate stock solutions showed the presence of negligible amounts of Na^+, therefore the SiP-TiO_2 particles were the only source of Na^+ ions in these isotherms. Closer examination showed that milliequivalent concentrations of Na^+ were being released as M^{n+} ions were sorbed onto the SiP-TiO_2 (ANa) particles. That is, when the concentration of Ce^{3+}, Sr^{2+} and Cs^+ sorbed by the SiP-TiO_2 were converted into millimol quantities and multiplied by their corresponding charge, i.e., millimol of charge, the obtained number was equal to the concentration of Na^+ released (Table 2). Once the sodium concentration plateaued [indicating all the sodium has been released (20 mg/L, Figure 5, b)], the previously sorbed Sr^{2+} and Cs^+ started to be released; thus, the latter ions acted as ion exchangers, allowing more Ce^{3+} to be taken out of solution as they are released.

Table 2. Millimol of charge (milliequivalent) of all three studied metals sorbed, or, in the case of sodium, released, at a specific concentration point in the isotherm in Figure 5 (b).

	Ce^{3+}	Sr^{2+}	Cs^{+}	Total	Na^{+}
10 ppm	0.44	0.46	0.2	1.1	1.22
20 ppm	0.855	0.9	0.1	1.86	1.73
70 ppm	1.92	0	0	1.92	1.73

Kinetic Model

The sorption rate of Ce^{3+} on SiP-TiO_2 (ANa) was calculated by using an initial Ce^{3+} concentration of 225 mg/g. As shown in Figure 5 (a), the kinetics were very fast, especially in the first five minutes, where 50% of the total Ce^{3+} metal sorbed was taken up. However, the process requires more than 3 h for equilibrium to be reached. This equilibrium time was slower than that reported for SiP ethyl analogue on SBA-15 and U^{4+}.[18] To obtain a clearer picture of the mechanism involved in the sorption process, this experimental data was put through both pseudo-first- and pseudo-second-order kinetic models. The linearised form of the rate equation by Lagergren was used to determine whether the kinetics were pseudo-first-order [Equation (1) in the Supporting Information]. In this equation, k_1 is the sorption rate constant (min^{-1}), while q_e and q_t are the amounts of metal sorbed in mg of metal per gram of SiP-TiO_2 (ANa) at equilibrium and at time (t), respectively. The plot of $(q_e - q_t)$ vs. t gave a straight line, and k_1 was calculated by calculating the slope (Table 3). The pseudo-second-order kinetic model was also applied; in this case both q_e and q_t had the same meaning as above and k_2 was the rate constant [g/mg/min; Equation (2) in the Supporting Information]. A plot of t/q_t vs. t was linear, and q_e and k_2 could be calculated from the slope and intercept, respectively. The model parameters and the correlation coefficient obtained for both equations are summarised in Table 3. Although both sets of results fit well with high R^2 values, the pseudo-second-order kinetic equation was found to have a higher R^2 value and its q_e value was closer to that observed experimentally.

Table 3. Kinetic model constants and correlation coefficients highlighting the sorption of Ce^{3+} onto SiP-TiO_2 (ANa).

	q_e (mg/g)	K_1 (min^{-1})	K_2 (g/mg/min)	R^2
Pseudo-fist-order	86.16	3.336×10^{-2}		0.997
Pseudo-second-order	92.59		9.84×10^{-4}	0.998
Experimental	92			

These results are consistent with the observations discussed in the previous section. That is, this system behaves as a chelating exchanger; therefore, it is no surprise that second-order-kinetics can be applied here. Because SiP-TiO_2 (ANa) has a porous structure, further investigation was carried out to determine whether diffusion steps were limiting factors with regard to the sorption process. A sorption process on porous solids can be broken down into four different stages; (i) bulk diffusion, (ii) film diffusion, (iii) intra-particle diffusion, and (iv) sorption (or ionic exchange) of the adsorbate on the surface. Because one or more of these processes are diffusion-limited steps, they may determine the rate and amount of material sorbed and they therefore must also be investigated.

The diffusion model is expressed by using the Weber and Morris equation; see Equation (3) in the Supporting Information. As before, q_t is the amount of metal sorbed at time t in mg/g. The constant k_{id} is the diffusion constant [mg/g/h]. A plot of q_t as a function of $t^{1/2}$ gives a straight line from which k_{id} can be found. The experimental kinetic data was applied to this equation, however, the points were not linearly distributed but, rather, give four straight lines with four different slopes. Similar kinetics were observed on the sorption of U^{6+} on DPTS (Ethyl SiP) functionalised SBA-15.[18] The initial steep-sloped portion represents bulk diffusion or exterior sorption rate, which is very high. The second and third portions can be attributed to intra-particle diffusion in the former, the outer "shell" of which was created by the hydrothermal process, and in the latter, the "core" TiO_2. Lastly, the fourth portion corresponds to the chemical equilibration of Ce^{3+} in SiP-TiO_2. Such kinetics suggests that intra-particle diffusion may play an important role in the rate determination in the sorption process but is not the sole rate-determining factor because of the deviation of the curves from the origin and because of the non-linear distribution of the plots.

Sorption Isotherm Model

Adsorption isotherms are fundamental to an understanding of the sorption mode of an adsorbate on a sorbent surface when equilibrium is attained. The Langmuir isotherm model used here to fit the experimental data is based on the assumption that the metal ions are sorbed as a monolayer, uniform and finite. It is also assumed that the sorption energy decreases as the distance from the surface increases. The linear form of the Langmuir isotherm can be expressed according to Equation (1); where C_e is the equilibrium concentration of adsorbate [mg/L], q_e represents the amount of adsorbed adsorbate at equilibrium [mg/g], and Q and b are the Langmuir constants related to sorption capacity [mg/g] and the affinity of the binding sites on sorbent (mL/mg), respectively. Q and b can be obtained by plotting C_e/q_e vs. C_e. Table 4 lists the parameters of the Langmuir model for the Ce^{3+} sorption on SiP-TiO_2 (ANa).

$$\frac{C_e}{q_e} = \frac{C_e}{Q} + \frac{1}{Q_b} \quad (1)$$

Table 4. Equilibrium concentrations of Ce/Nd, Ce/Gd and Ce/Yb solutions sorbed onto SiP-TiO_2 (ANa) in millimol of metal sorbed per gram of SiP-TiO_2. Ratio of Ce^{3+} to M^{3+} sorbed is also shown.

Ce	Nd	Gd	Yb	Ratio
0.428	0.44			1:1.02
0.495		0.656		1: 1.325
0.335			0.479	1:1.429

With a correlation coefficient of 0.9998 and the fact that the equilibrium sorption capacity (Q) obtained from the

Langmuir model (92.59 mg/g) is practically identical to the experimentally observed saturation capacity (92.98 mg/g), it can be concluded that the sorption of Ce^{3+} onto SiP-TiO_2 follows the Langmuir sorption model. According to the Langmuir model, the favourability of SiP-TiO_2 (ANa) as a Ce^{3+} sorbent, related to the separation factor R_L, can be obtained from the Langmuir sorption constant, Equation (2), where C_0 is the initial metal ion concentration.

$$R_L = \frac{1}{1 + bC_0} \quad (2)$$

A value of $0 < R_L < 1$ indicates that the sorbent is a favourable medium for the sorption of the given metal ion. The calculated R_L value was found to be between 8.6×10^{-3} and 9.3×10^{-4}, thus, the SiP-TiO_2 (ANa) can be considered a favourable sorbent for Ce^{3+}. The affinity of the SiP ligand for Ce^{3+} (ΔG_L), was also calculated from this data and was found to be –17309 J/mol (Table 5).

Table 5. Isotherm model constants and coefficients for cerium, gadolinium and ytterbium.

	Q (mg/g)	b (mL/mg)	R^2	Exp. (mg/g)	ΔG_L (J/mol)
Ce	92.59	12	0.9998	92.98	–17309
Gd	120.48	41.5	0.9996	121.17	–21022
Yb	138.8	360	0.9997	138.01	–26705

Lanthanide Separation

The ability of SiP-TiO_2 (ANa) to separate Ce^{3+} from other L^{3+} ions was also examined. Nitrates of Nd^{3+}, Gd^{3+}, and Yb^{3+} were chosen for these studies because of their charge (M^{3+}) and their increasing atomic mass. To carry out these tests, mixed solutions of Ce^{3+} and the other lanthanides were prepared. To these stock solutions (Ce/Nd, Ce/Gd and Ce/Yb), was then added a dispersion of SiP-TiO_2 (ANa). The same procedure described for the kinetic experiments was used for these studies. The results of these experiments are presented in Table 4, which shows the equilibrium points of these experiments in millimol of metal per gram of SiP-TiO_2 (ANa), as well as the ratio of M^{3+} to Ce^{3+}. Again, a large amount of metal was sorbed within the first five minutes. The Ce^{3+}/Nd^{3+} mixture showed an almost identical equilibrium concentration for both metals, which is not surprising because Ce^{3+} and Nd^{3+} have very similar atomic radii and atomic masses. However, the Ce^{3+}/Gd^{3+} and Ce^{3+}/Yb^{3+} mixtures did show some degree of separation. In fact, as the atomic weight of the competitor lanthanide increased so too did its uptake.

The ratio of Ce/Nd sorbed was almost 1:1, however, the ratio of Ce/Gd sorbed was higher (1:1.3). This difference in sorbance continued to increase with atomic weight, and a sorbtion ratio of 1:1.4 was observed for the Ce/Yb mixture. These results suggested that as the difference in weight between the metal ions increases so too does the ability of the SiP-TiO_2 (ANa) to separate them. Langmuir adsorption isotherms were also individually carried out on $Gd(NO_3)_3$ and $Yb(NO_3)_3$, as described earlier (Figure 5, b). By comparing Tables 4 and 5 it can be seen that there is an increase in both the Langmuir constants (Q and b) and the absolute ΔG_L values for SiP-TiO_2 (ANa) as the atomic weight of the target lanthanide increased. We therefore submit that this material could be used in the liquid/solid separation of Lanthanides depending on whether they are light or heavy Ln.

Metal Recovery

A series of simple experiments were also performed on the lanthanide-loaded SiP-TiO_2 (ANa) particles. The metal loaded particles were stirred in various acid solutions (HNO_3, H_2PO_4 or HCl) for 2 h, changing the acid solution after 1 h. ICP analysis was then used to determine the presence and concentration of any desorbed metal ions. In this way it was found that ca. 80% recovery of the sorbed metals was possible. This result was independent of the type of acid used. Furthermore, the full concentration of recoverable metal was present in the first solution after 15 min. The collection and redispersal of the particles in a second acid solution after the first hour resulted in little or no additional metal ions being recovered.

Counter-Ion Tests

To investigate the effect on SiP-TiO_2 (ANa) of changing the counterion, a solution of Gd and Sr chloride was prepared. This solution was then stirred with SiP-TiO_2 (ANa) (as in previous experiments) and the results were examined. Again, no Sr^{2+} was sorbed by the time the equilibrium point was reached. The use of either $GdCl_3$ or $Gd(NO_3)_3$ as the Gd source made very little difference to the overall profile of the sorbance curve. The equilibrium concentration of Gd was slightly higher when $GdCl_3$ was used as the Gd source {[$Gd(NO_3)_3$] 0.744 mm/g vs. [$GdCl_3$] 0.795 mm/g}, however, this difference was well within the bounds of experiment error. Therefore, the type of counterion used seems to have little effect on the sorption process under these experimental conditions.

Conclusions

A novel sorbent composed of phosphonate-functionalised mesoporous titania was synthesised by the co-condensation method and used in Ln^{3+} sorption, in batch processes. The sorption of Ln^{3+} on SiP-TiO_2 (ANa) was studied as a function of various parameters such as time, pH, and Ln^{3+} concentration. The initial kinetics of Ln^{3+} sorption on SiP-TiO_2 (ANa) is ultra-fast, with 50% of the total amount of metal being sorbed in the first minute or two. However, the equilibrium time is over 3 h. The sorption of Ce^{3+} was found to follow pseudo-second-order type sorption kinetics. Intraparticle diffusion plays an important role in the sorption processes but it could not be accepted as the sole rate-determining step. The measured maximum sorption capacity depends on the metal examined, starting with Ce at 92 mg/g and increasing with the atomic weight

of the lanthanide. The sorption isotherms for Ce^{3+}, Gd^{3+} and Yb^{3+} have been successfully modelled by the Langmuir isotherm, which revealed a monolayer chemical sorption. The sodium-washed SiP-functionalised TiO_2 demonstrated some ability to separate Ln^{3+} metals according to molecular mass. Finally, it was noted that changing the counterion from nitrate to chloride had little effect on the profile or equilibrium concentration of the sorption of Gd^{3+}. Finally, simple recovery tests were performed by dispersing the particles in various acids, HNO_3·H_2PO_4 and HCl. It was found that ca. 80% of the sorbed metal could be recovered.

Experimental Section

Materials: Dimethylphosphatoethyltriethoxysilane (SiP) was provided by our industrial partners Specific Polymers. Ethylene glycol ($HOCH_2CH_2OH$) and titanium(IV) isopropoxide {$Ti[OC(CH_3)_2]_4$} were obtained from Sigma–Aldrich. All metal nitrates, with the exception of $Yb(NO_3)_3$·xH_2O (Fluka), were also purchased from Sigma–Aldrich. All these materials were used as received. Because AES-ICP was used as the main tool to determine metal concentration, all nitrate stock solutions had a metal concentration of 20 ppm [mg/L] or less. Deionised water was prepared by using a Sartorius water system (18.2 MΩ·cm). All sonication was carried out with a VWR ultrasonic cleaner (USC100T).

Preparation of SiP-Functionalised TiO_2: Functionalised TiO_2 was prepared by using a reported method, which was modified to include the SiP functionalising molecule.[27] Briefly, $Ti[OCH(CH_3)_2]_4$ (5 g) and SiP (0.8 g) were weighed out and mixed well together. This mixture was then poured into ethylene glycol (50 g) under constant stirring. The solution turned a vivid milky-white immediately on addition of the Ti/SiP mixture. The resulting milk-white solution was stirred overnight, after which the white colour disappeared and the solution was once again clear and colourless. The Ti/SiP ethylene glycol solution was then poured into acetone (250 mL) under constant stirring. The white colour reappeared and strengthened over time. After 2 h stirring at room temperature, the SiP-TiO_2 dispersion was heated to 60 °C and stirred for 6 h at 60 °C and for an additional 14 h at 40 °C. The particles were collected by centrifugation and washed several times first with ethanol and then with water, then they were dried overnight at 40 °C and washed in a Soxhlet with ethanol for 18 h. The Soxhlet extracted (AS) particles were dried (40 °C overnight) then transferred to a 500 mL round-bottomed flask and deionised water (350 mL) was added. The contents were sonicated until the particles were thoroughly dispersed and then stirred vigorous and heated to reflux for 6 h. These hydrothermal treated (AH) particles were then collected by decanting and centrifugation, washed several times in deionised water and oven-dried at 40 °C. The particles were then dispersed in aq. NaOH (15 g/L, 150 mL) and stirred for 1 h, then collected by centrifugation and washed with deionised water until pH neutral. The particles were again dried at 40 °C overnight. Note: Unfunctionalised TiO_2 was prepared as reported[29] and as above with the only difference being the absence of SiP.

Sorption Experiments: All sorption studies were carried out in deionised water. For the kinetic experiments, 100 mL of ca. 20 ppm solutions of the target metals were prepared under constant stirring. Separately, 20 mg of SiP-TiO_2 or TiO_2 were sonicated in deionised water (20 mL) until a homogeneous dispersion was acquired. To start the kinetic experiment these 20 mL Titania dispersions were added to metal nitrate solutions (100 mL) with the timer being started immediately upon addition. Samples (7 mL) were taken at defined intervals and immediately passed through a Whatman 200 nm syringe filter to remove the TiO_2. The concentration of the remaining metal in the filtered solution was then determined by AES-ICP analysis.

Langmuir isotherms were determined by using the same stock solution concentration as described above (20 ppm metal). Each isotherm contained 10 points/experiments with each point being a different dilution of the stock solution; starting with 2 ppm of metal and the final point being the stock solution itself, i.e., 20 ppm. Each point consisted of 20 mL of these solutions with 4 mg of sorbent. All samples were sonicated for 30 min to ensure homogeneous dispersion and then stirred for 20 h. Again Whatman 200 nm syringe filters were used to stop the sorption process and the remaining metal concentration in solution was determined by using ICP-AES analysis.

Analytical Techniques: The morphologies of the samples were observed with an ESEM-FIG (FEI Quanta 200). The N_2 sorption-desorption isotherms were measured at –196 °C with a micromeritics ASAP 2020 Surface Area and Porosity Analyser. The sample was degassed at 80 °C overnight. The surface area was calculated by the Brunauer–Emmett–Teller (BET) method, and the pore size was calculated from the maximum of the pore size distribution curve calculated by the Barrett–Joyner–Halenda (BJH) method using the sorption branch of the isotherm. The total pore volume was calculated by the single point method. ^{13}C and ^{31}P and ^{29}Si CP/MAS NMR were measured with a Bruker 400 MHz NMR spectrometer operating at 100 MHz and a sample spinning frequency of 12 kHz. Metal concentration, with the exceptions of sodium and caesium was determined with a Spectro Arcos ICP-OES spectrometer. Cs and Na concentration were determined using an ion chromatograph (Dionex ICS 5000 with an ICS Series AS-AP autosampler).

Supporting Information (see footnote on the first page of this article): SAXS and N_2 isotherm absorption measurements of the unfunctionalised TiO_2 (BH) and (AH) as well as the functionalised SiP-TiO_2 (BH), (AH) and (ANa). ^{29}Si MAS-NMR spectra of SiP-TiO_2 (ANa) and liquid ^{31}P NMR spectra of the SiP ligand. Further sorption data comparing the unfunctionalised TiO_2 vs. SiP TiO_2 (AH) and (ANa) is also available, as well as data comparing functionalised and unfunctionalised SBA-15 and TiO_2.

Acknowledgments

The authors would like to acknowledge the assistance and to thank Cyrielle Rey (LNER ICSM Marcoule), for all her help throughout this project. Thanks to Johann Ravaux (LM2E, ICSM, Marcoule) for providing the SEM measurements. The solid-state NMR measurements were performed at the ICGM Montpellier by Philippe Gaveau and Christine Biolley. Liquid NMR analysis of SiP was provided in house (ICSM LTSM) by Raphaël Turgis. The authors would also like to especially thank Dr Ania Selmi and Dr Matthew Manktelow for their assistance in editing this work. This work was carried out under the financial assistance of the CEA (Commissariat à l'énergie atomique et aux énergies alternatives). Dimethyl 2-(triethoxysilyl)ethylphosphonate (SiP) [17940-10-2] was provided by Specific Polymers www.specificpolymers.fr under the reference SP-3-12-001.

[1] A. C. Jones, H. C. Aspinall, P. R. Chalker, *Surf. Coat. Technol.* **2007**, *201*, 9046–9054.

[2] Z. V. P. Murthy, A. Choudhary, *Desalination* **2011**, *279*, 428–432.
[3] K. Chaudhury, K. N. Babu, A. K. Singh, S. Das, A. Kumar, S. Seal, *Nanomedicine* **2013**, *9*, 439–448.
[4] M. Eski, F. Ozer, C. Firat, D. Alhan, N. Arslan, T. Senturk, S. Işik, *Burns* **2012**, *38*, 283–289.
[5] J. Christoffers, T. Werner, M. Rössle, *Catal. Today* **2007**, *121*, 22–26.
[6] P. Maestro, D. Huguenin, *J. Alloys Compd.* **1995**, *225*, 520–528.
[7] L. Zhang, W. Li, X. Hu, Y. Peng, J. Hu, X. Kuang, L. Song, Z. Chen, *Prog. Nat. Sci.* **2012**, *22*, 488–492.
[8] H. Hasannejad, T. Shahrabi, M. Jafarian, *Mater. Corros.* **2013**, *64*, 1104–1113.
[9] X.-L. Zheng, Y. Liu, M. Pan, X.-Q. Lü, J.-Y. Zhang, C.-Y. Zhao, Y.-X. Tong, C.-Y. Su, *Angew. Chem. Int. Ed.* **2007**, *46*, 7399–7403.
[10] Z. Xiao, G. Cheng, T. Zhang, F. Xu, *Surf. Coat. Technol.* **2000**, *128–129*, 461–464.
[11] I. V. Melnyk, V. P. Goncharyk, L. I. Kozhara, G. R. Yurchenko, A. K. Matkovsky, Y. L. Zub, B. Alonso, *Microporous Mesoporous Mater.* **2012**, *153*, 171–177.
[12] P. K. Leung, C. Ponce-de-León, C. T. J. Low, A. A. Shah, F. C. Walsh, *J. Power Sources* **2011**, *196*, 5174–5185.
[13] *Catalysis by Ceria and Related Materials* (Ed.: A. Trovarelli), Imperial College Press, **2002**.
[14] C. R. Hammond (Ed.), *The Elements*, in: *Handbook of Chemistry and Physics*, 81st ed., **2000**, CRC Press,.
[15] G. M. Laila Manji, Carl Firman, in: *Geopolitical Analysis Quarterly*, VM Group, London, **2011**.
[16] H. Tabuchi, in: *New York Times*, New York, **2010**.
[17] a) C. Calmon, *Chem. Eng.* **1980**, *87*, 271–274; b) G. Dupouy, I. Bonhoure, S. Conradson, T. Dumas, C.Hennig, C. Le Naour, P. Moisy, S. Petit, A. Scheinost, E. Simoni, C. Den Auwer, *Eur. J. Inorg. Chem.* **2011**, 1560–1569.
[18] L.-Y. Yuan, Y.-L. Liu, W.-Q. Shi, Y.-L. Lv, J.-H. Lan, Y.-L. Zhao, Z.-F. Chai, *Dalton Trans.* **2011**, *40*, 7446–7453.
[19] O. A. Dudarko, V. P. Goncharik, V. Y. Semenii, Y. L. Zub, *Protection of Metals* **2008**, *44*, 193–197.
[20] J. Yong Gang, Q. Shi Zhang, X. Zhi Ping, Y. Zhimin, H. Yining, J. C. D. da Costa, L. Gao Qing, *J. Mater. Chem.* **2009**, *19*, 2363–2372.
[21] Y. Pan, H. G. Tsai, J. G. Jiang, C. Kao, T. Sung, P. Chiu, D. Saikia, J. Chang, H. Kao, *J. Phys. Chem. C* **2012**, *116*, 1658–1669.
[22] P. Dutournié, L. Limousy, S. Déon, P. Bourseau, *Desalination* **2011**, *265*, 184–189.
[23] N. Kallay, D. Babić, E. Matijević, *Colloids Surf.* **1986**, *19*, 375–386.
[24] M. J. Comarmond, T. E. Payne, J. J. Harrison, S. Thiruvoth, H. K. Wong, R. D. Aughterson, G. R. Lumpkin, K. Mueller, H. Foerstendorf, *Environ. Sci. Technol.* **2011**, *45*, 5536–5542.
[25] G. D. Panagiotou, T. Petsi, K. Bourikas, C. S. Garoufalis, A. Tsevis, N. Spanos, C. Kordulis, A. Lycourghiotis, *Adv. Colloid Interface Sci.* **2008**, *142*, 20–42.
[26] K. E. Engates, H. J. Shipley, *Environ. Sci. Pollut. Res. Int.* **2011**, *18*, 386–395.
[27] T. Tsuru, D. Hironaka, T. Yoshioka, M. Asaeda, *Desalination* **2002**, *147*, 213-216.
[28] T. Tsuru, D. Hironaka, T. Yoshioka, M. Asaeda, *Separation Purification Technol.* **2001**, *25*, 307–314.
[29] S. Li, Q. Shen, J. Zong, H. Yang, *J. Alloys Compd.* **2010**, *508*, 99–105.
[30] X. Jiang, T. Herricks, Y. Xia, *Adv. Mater.* **2003**, *15*, 1205–1209.
[31] G. Guerrero, P. H. Mutin, A. Vioux, *Chem. Mater.* **2001**, *13*, 4367–4373.
[32] X. Zhang, T. Ma, Z. Yuan, *J. Mater. Chem.* **2008**, *18*, 2003–2010.
[33] T. R. D. Hoebbel, H. Schmidt, *J. Sol-Gel Sci. Technol.* **1995**, *2*, 139–149.
[34] A. Cardenas, N. Hovnanian, M. Smaihi, *J. Appl. Polym. Sci.* **1996**, *60*, 2279–2288.
[35] M. D. Tsai, S. L. Huang, J. F. Kozlowski, C. C. Chang, *Biochemistry* **1980**, *15*, 3531–3536.

Received: January 9, 2014
Published Online: March 27, 2014

